Nanosheet Synthesis of Metal Organic Frameworks in a Sandwich-Like Reaction Field for Enhanced Gate-Opening Pressures

Takeru Omiya, Koki Sasaki, Yoshiaki Uchida, Norikazu Nishiyama*

Graduate School of Engineering Science, Osaka University, Toyonaka, Osaka 560-8531 (Japan)

E-mail: yuchida@cheng.es.osaka-u.ac.jp

Keywords: nanosheet; liquid crystal; metal organic framework; gas adsorption

ABSTRACT

Elastic layer-structured metal-organic frameworks (ELMs) are a family of flexible nano-porous metal organic frameworks (MOFs) showing gate-opening gas adsorption. The gate-opening pressure shifts to a higher value by crystal downsizing. However, the MOF nanoparticles and nanorods showing the gate-opening gas adsorption grow more than 50 nm even for their shortest sides. Here we describe the synthesis and unique gas adsorption behavior of the first example of nanosheets of ELMs (ELM-NSs). The thickness and horizontal width of the ELM-NSs obtained from a new synthetic method using the inside the bilayers in hyperswollen lyotropic lamellar

(HL) phases as sandwich-like reaction fields (SRFs) are a few nanometers and several hundreds of nanometers, respectively. The previously reported rationalization of the temperature dependence of the gate-opening pressures for ELMs enables us to discuss the size effects in terms of the adsorption-induced structural transitions and the Helmholtz free energy change of the host.

Surfaces and interfaces of materials show far different physical and chemical properties from bulk properties of the same materials. The unique properties are especially pronounced in materials only with surfaces: nanowires and nanosheets (NSs). NSs are two-dimensional (2-D) materials with a thickness of a few or tens of nanometers, and thus, NSs are not only ultra-lightweight but also flexible.[1] Since the first NS was obtained by exfoliating a natural laminated compound, smectite,[2] numerous thin (several nm) NSs have been synthesized in the same way:[3-5] graphite, mica, and so on.[6-8] For the synthesis of NSs of non-exfoliable materials, 2-D growth on a smooth and chemically specific substrate has been alternatively used; however, the products from most of the bottom-up methods are thicker (several tens of nanometers) than those formed by the top-down exfoliation methods.[9] Meanwhile, the top-down methods to give thinner NSs are applicable to specific materials.[9] To resolve the dilemma, a variety of improved methods have been proposed; e.g., gold NSs have been prepared by several routes, such as the reduction of chloroaurate ions with organic acids,[10] and electrochemical,[11] photoreduction,[12] microwave-polyol reduction,[13] and thermal reduction methods.[14] The synthesis of gold NSs is also possible in an anisotropic hexadecylglyceryl maleate hydrogel composed of highly dispersed bilayers as a 2-D scaffold;[9] the 2-D scaffold is composed of the amphiphilic molecules with hydroxyl groups, with which Au^{3+} ion specifically interacts. However, because the bilayers are several hundreds of

nanometers apart from each other, the materials can grow perpendicularly outwards from the bilayers. To satisfy both the extreme thinness and the wide range of applicable materials, we have recently proposed a new method to synthesize NSs by using a hyperswollen lyotropic lamellar (HL) phase composed of bilayers of a non-ionic amphiphile.[15] The accumulation and reaction of hydrophobic or hydrophilic ingredients in the thin hydrophobic or hydrophilic region inside the bilayers several hundreds of nanometers apart from each other in the HL phases of aqueous or organic amphiphilic solutions should result in sufficiently dispersed very thin hydrophobic or hydrophilic NSs. In fact, hydrophobic polystyrene NSs have been successfully synthesized in the thin hydrophobic regions in the sandwich-like reaction fields (SRFs) inside the bilayers of HL phases of aqueous amphiphilic solutions.[15] In principle, the SRF method using HL phases could be applied to any hydrophobic and hydrophilic non-exfoliable materials. As the next target of the NS synthesis using the SRF method to extend the range of the applicable materials, metal organic frameworks (MOFs) with three-dimensional (3-D) networks are suitable because they are non-exfoliable materials made from both hydrophilic and hydrophobic ingredients.

Some MOFs are categorized into a family of hybrid nano-porous materials that are formed by the coordination of metal ions with organic ligands. In particular, pores and cavities in MOFs with 3-D networks have potential in industry: gas storage, gas separation, catalysis and nanoscale reaction systems. In addition, MOFs with 3-D networks can be scaled down to nanometer size, which makes them potentially useful as nanocarriers in medical applications.[16] MOF nanoparticles have previously been produced by physical or chemical growth inhibition; e.g., microwaves and ultrasounds induce rapid nucleation to decrease the mean size of the particles, and alternative ligands added as a modulator to block the growth of the particles.[16,17] These

methods are called coordination modulation methods. A similar approach also enables to synthesize MOF nanorods.[18] Recent investigations have demonstrated that coordination modulation of twofold interpenetrated frameworks of $[Cu_2(dicarboxylate)_2(amine)]_n$ with 3-D networks regulates the structural flexibility and induces a shape-memory effect in the coordination frameworks.[19] However, the mechanism of the size-dependence of the shape-memory effect is not clear, and the MOF nanoparticles and rods by these methods grow more than 50 nm even for the shortest sides. For exfoliable MOFs with 2-D networks, the NSs are also available by several methods; the synthetic procedures include liquid/liquid or gas/liquid interfacial synthesis, chemical vapor deposition, and liquid-phase exfoliation,[20,21] but these methods are not applicable to MOFs with 3-D networks. The above-mentioned SRF method using HL phases could be promising for the synthesis of NSs for the MOFs with 3-D networks.[15]

As a family of functional MOFs with 3-D networks, elastic layer-structured metal–organic frameworks (ELMs) have been well studied;[22-25] the 2D layers in ELMs are hydrogen-bonded with each other, and therefore, we think that ELMs are 2D-layered 3D MOFs. They are the first soft porous crystals (SPCs) showing gate-opening gas adsorption owing to the shape-memory effect.[19,26] The gate-adsorption is accompanied with expansion/shrinkage structural modulation. However, it is not the origin of the gate-opening behavior but the result. Very recently, one of NSs of ELMs (ELM-NSs) were successfully synthesized by exfoliation.[27] However, as the next target of the NS synthesis using the SRF method to extend the range of the applicable materials, ELM-NSs are suitable because they are synthesized from both hydrophilic and hydrophobic ingredients. Here, we report the synthesis of the ELM-NSs containing Cu^{2+} ion (ELM-11 $[Cu(bpy)_2(BF_4)_2]$ and ELM-13 $[Cu(bpy)_2(CF_3BF_3)_2]$) with large areas and well-tuned thicknesses ranging from a few to several tens of nanometers by the SRF method using HL phases and

discuss the size dependence of the gate-opening gas adsorption of the ELM-NSs in terms of the adsorption-induced structural transitions.

Because ELMs are water-insoluble MOFs, aqueous amphiphilic solutions showing HL phases could be applicable to ELMs. The addition of the hydrophilic Cu^{2+} and counter ions to the HL phases with the hydrophobic ligand of ELMs, 4,4'-bipyridine (bpy), in the hydrophobic regions would result in the thin NSs of ELMs. As described in reference 15, aqueous solution of $C_{12}E_6$ should also be suitable in this case. Although simple aqueous solution of $C_{12}E_6$ does not show any HL phases because the hydrophobic region is too small to stabilize the bilayers, hydrophobic additives can stabilize HL phases of the aqueous solution of $C_{12}E_6$. Naturally, bpy could also stabilize the HL phases of aqueous $C_{12}E_6$ solution and generate a periodically ordered structure with thick aqueous region (**Figure 1a**). In fact, after stirring the aqueous $C_{12}E_6$ solution dissolving bpy ($C_{12}E_6$-bpy solution), iridescent colors typical of HL phases[27] emerge, and the reflectance spectra measured according to reference 29 indicate that the $C_{12}E_6$-bpy solutions exhibit HL phases; e.g., the $C_{12}E_6$-bpy solution with the solute concentration of 2.3 wt % shows the HL phase between 42 and 58 °C. Furthermore, it suggests that bpy is in the hydrophobic regions inside the bilayers.

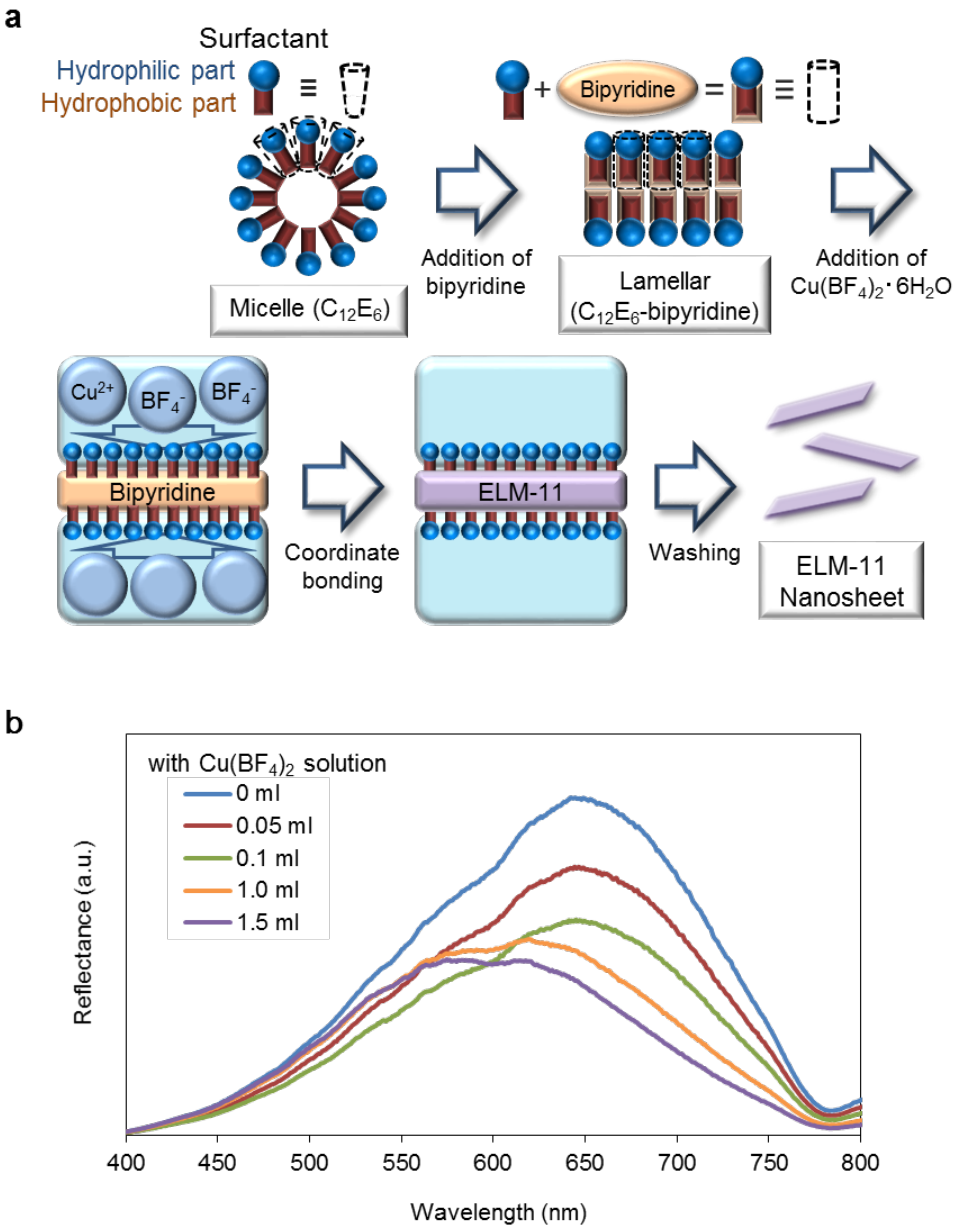

Figure 1. Schematic illustration of the synthesis procedure for the NSs of ELM-11. Aqueous $C_{12}E_6$ solutions intrinsically do not show any HL phases due to the packing parameter of $C_{12}E_6$. When a hydrophobic compound is introduced in a $C_{12}E_6$ solution, the hydrophobic part of self-assembly structures practically increases. As a result, the HL phase is stabilized. For the synthesis of the NSs of ELM-11, bipyridine works as the stabilizing hydrophobic additive. (b) Reflectance spectroscopy of $C_{12}E_6$ solution. Reflection spectra of a $C_{12}E_6$-bpy solution after

addition of 1.5 ml $Cu(BF_4)_2$ recorded at various injection. The spectra were differential spectra between the spectra of a sample stirred at 300 rpm and those of the same sample unstirred.

Next, we tried to synthesize the ELM-NSs using the SRF method; aqueous copper salt solutions are added to the $C_{12}E_6$-bpy solution. The obtained solution has no precipitates, and therefore, the obtained ELM-NSs are likely to be well dispersed in the HL phases. When we observed the contents of the solutions by TEM, we found NS materials as shown in **Figure 2a**. The thickness and horizontal width of the ELM-NSs measured by AFM are a few nanometers and several hundreds of nanometers, respectively, as shown in **Figure 2b**. To compare the difference in the structure between the obtained ELM-11-NS and commercially available ELM-11, we measured XRD patterns for them at 195 K as shown in **Figure 2c**. The XRD pattern of ELM-11 fitted the previously reported pattern, though we cannot decide the crystal lattice.[30] Comparing with the XRD pattern of ELM-11, the peaks around 14.5°, 17.5° and 19° disappeared in that of ELM-11-NS. These peaks are likely to originate from the periodicity of the thinnest direction. The peak around $2\theta = 22^\circ$ is slightly shifted to higher diffraction angle for ELM-11-NS; one of the layer spacings is likely to decrease. The reason of the shift of the peak around $2\theta = 12^\circ$ is the same as that around $2\theta = 22^\circ$. The decrease of the layer spacings could occur due to lattice relaxation, in which the lattice constants gradually decrease at surfaces of crystals, because NSs have large specific surface area. In a previously reported paper, when the interlayer distance decreases with a decrease in temperature, the gate-opening pressure increases.[31] In our case, the layer spacing of ELM-11 was estimated to be 0.408 nm, whereas that of the ELM-11-NS was calculated as 0.406 nm. The reduction of the layer spacing is 0.49 %, and it can be expected to similarly affect the gate-opening pressure.

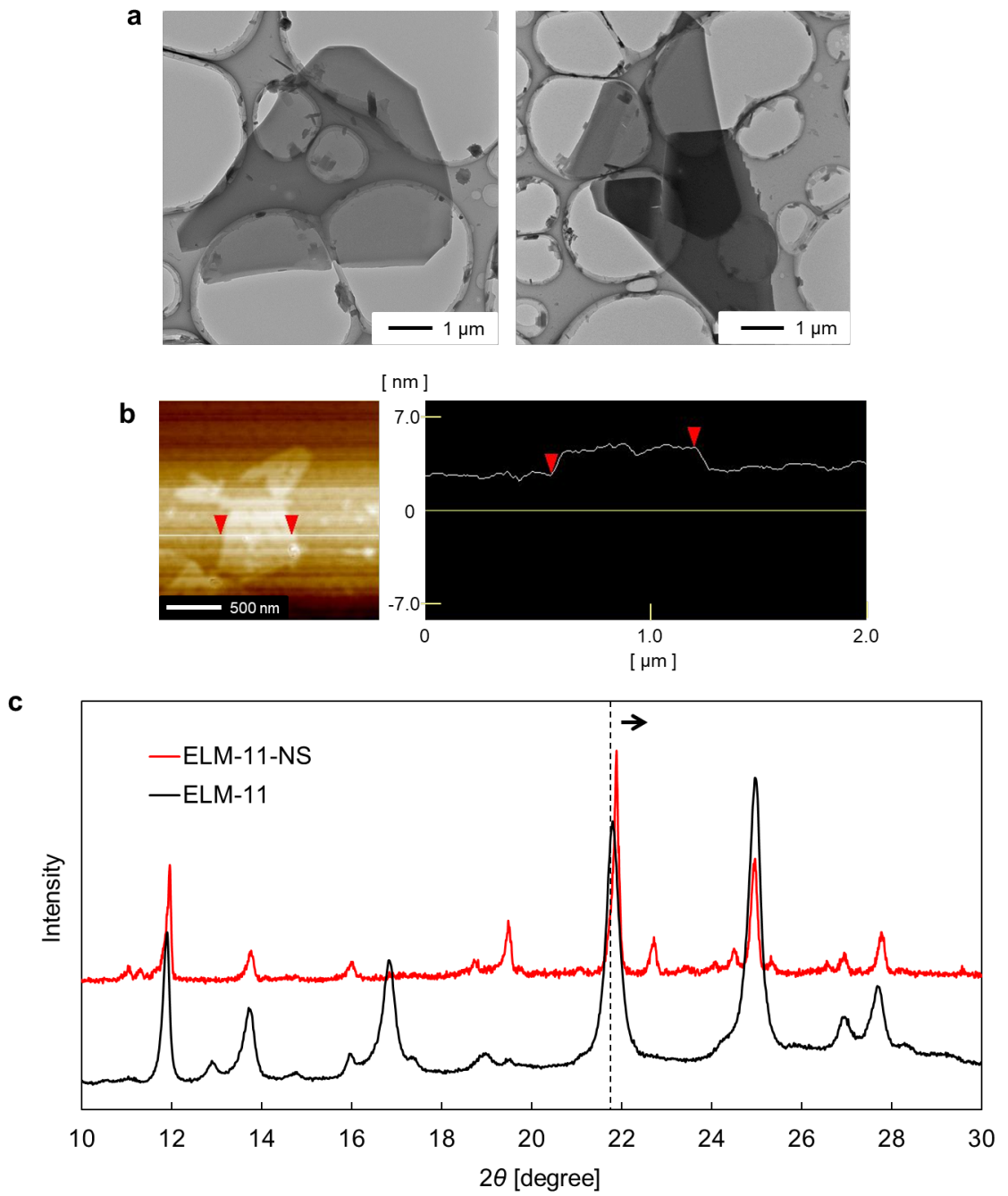

Figure 2. Synthesized ELM-11-NSs. (a) TEM photograph of one of the synthesized NS of ELM-11. (b) AFM photograph and cross section of one of the synthesized NS of ELM-11. These indicate that the thickness and horizontal width of the synthesized NS of ELM-11 are several nanometers and several hundreds of nanometers, respectively. (c) XRD patterns of ELM-11 and ELM-11-NS at 298 K.

To examine whether the ingress of hydrophilic ions into the hydrophobic SRFs occurs for the synthesis of the ELM-NSs in the hydrophobic region inside the bilayers, we discuss the change of the reflection spectrum of the HL phases of $C_{12}E_6$-bpy solution when the hydrophilic copper(II) tetrafluoroborate ($Cu(BF_4)_2$) is added to synthesize NSs of ELM-11. The reflection spectrum of $C_{12}E_6$-bpy solution (**Figure 1b**) without any copper salt shows a peak at 642 nm, indicating the formation of an ordered structure with a periodic distance on the order of submicrometers throughout the whole system. According to the Bragg equation ($\lambda = 2nd \sin \theta$, where n, d, θ, and λ are the refractive index of water, the periodic spacing, the angle of incidence, and the wavelength of the reflected light, respectively), the periodic spacing between adjacent $C_{12}E_6$-bpy bilayers is estimated to be 246 nm. As the concentration of the copper salt increases, the reflection intensity decreases but the reflection peak stayed at the same wavelength. Therefore, the decrease of the reflection intensity indicates that the HL region with the periodically ordered structure of the system contracts because the hydrophobic NSs of ELM-11 coated with $C_{12}E_6$ are not incorporated into the HL system.

The obtained ELM-NSs should exhibit gate-opening gas adsorption different from their bulk states. As the thickness decreases to several nanometers, the gate-opening pressure could shift to the highest value so far. In fact, the nitrogen adsorption isotherms of the ELM-NSs show the characteristic sharp uptake of N_2 on the NSs of ELM-11 and ELM-13 at relative pressures (P/P_0) of 0.4 and 0.8 as shown in **Figure 3a** and Supporting Information, which are much larger than those for the bulk samples (0.15 and 0.4), respectively. The shift of the gate-opening pressures supports the decrease of layer spacings that the observed peak shift in the XRD pattern indicates. In addition, the decrease of layer spacings sometimes occurs due to lattice relaxation as

mentioned above. Furthermore, the total amounts of adsorbed N_2 on the NSs of ELM-11 and ELM-13 are 1.6 and 4.4 times smaller than that on their bulk states. The experimental results also suggest that the gate-opening pressure is controllable only by the one-dimensional (1-D) thickness. Recent investigation rationalized the temperature dependence of the gate-opening gas adsorption of SPCs in terms of Helmholtz free energy of the host SPCs change during the adsorption.[31] According to this theory the gate-opening pressure value depends on the chemical potential of the SPCs adsorbing gas molecules and the temperature. In the present case, although temperature is constant, the effect of the crystal downsizing of ELMs is similar in the layer spacing to that of the cooling of ELMs. The layer compression could have an influence on the chemical potential of the ELMs, and thus, the gate-opening pressure would increase. The above-mentioned theoretical calculation[31] suggests that the gate-opening pressure is independent of the free energy of guest molecules. In fact, the adsorption isotherms for CO_2 also show the increase of the gate opening pressures as shown in **Figure 3b**. It indicates that the control of the thickness of SPC-NSs by using the SRF method would enable the control of the gate-opening pressures.

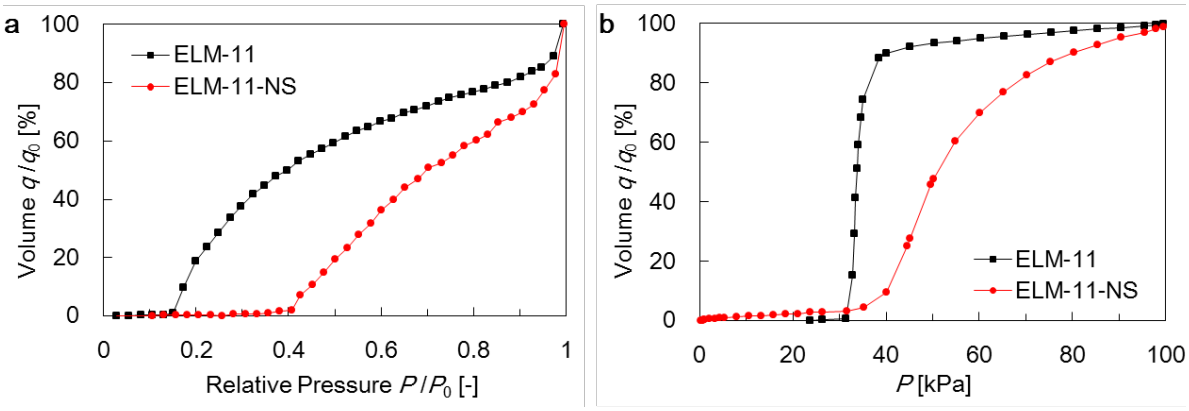

Figure 3. N_2 and CO_2 adsorption isotherms of bulk sample and NSs of ELM-11. (a) Adsorption isotherms of N_2 on the bulk sample of ELM-11 (produced by TCI) (black square) and the synthesized NSs of ELM-11 (red circles) at 77 K. We obtained the nitrogen adsorption isotherm

of the products and observed the characteristic sharp uptake of the NSs of ELM-11 at P/P_0 =0.4, or gate-opening pressure (P/P_0 is relative pressure) regardless of almost nil adsorption below the gate-opening pressure. As a result, we elucidated that the gate-opening pressure depends on crystal downsizing of ELM-11. STP means standard temperature and pressure. (b) We performed carbon dioxide adsorption measurements at 273 K on the NSs of ELM-11. These experiments also suggested that the gate-opening pressure is controllable by the crystal size.

We have successfully synthesized the suspension of the ELM-NSs, which have been extremely difficult to be produced so far. The thickness and horizontal width of the ELM-NSs are a few nanometers and several hundreds of nanometers, respectively. We also measured the reflection spectrum of the HL phases of $C_{12}E_6$-bpy solution when the hydrophilic copper salts are added. These results indicate that the periodically ordered structures of the system could be maintained during the reaction process. In addition, we observed blue shift of the spectrum, and we would like to discuss the blue shift by using complete spectroscopic data in another paper with the data obtained from a laser diffraction particle size analyzer. We then performed N_2 and CO_2 adsorption measurements, and demonstrated that the gate-opening pressure depends on the thickness. Our results indicate that we can discuss the size dependence of the gate-opening gas adsorption of the SPCs in terms of their Helmholtz free energy changes during the adsorption-induced structural transitions. The discussion of the change of the adsorption behavior is likely to be useful as an evidence of the formation of ELM-11-NS.

EXPERIMENTAL SECTION

Materials. Hexaethylene glycol monododecyl ether ($C_{12}E_6$) (0.18 g) and bpy (0.025 g) were dissolved in deionized water (8.8 g). The solution was stirred at 300 rpm by a magnetic stirrer

with length of 20 mm and diameter of 7 mm at 54ºC. After stirring the solution, iridescent colors emerge; this is typical of HL phases.[28] Addition of an aqueous solution (1 ml) of hydrated copper(II) tetrafluoroborate (0.10 M) or hydrated copper(II) tetrafluoroborate (0.05 M) and potassium (trifluoromethyl)trifluoroborate (0.05 M) for ELM-11 or ELM-13 gave a solution with little blue precipitate. After 15 min stirring, the blue precipitates were collected by dried for 1 day at 75 ºC and were then washed with ethanol. The products were dried under reduced pressure for 2 h.

XRD measurement. The crystal structure of the products was identified by X-ray diffraction (XRD) measurement recorded on a PANalytical X'Pert-MPD diffractometer using Cu-Kα radiation. The scan range was from 5 º to 40 º (2 theta) at 1 º /min.

Reflectance spectroscopy. Experimental setup for the reflectance spectroscopy is the same as that used in reference 15. To remove scattering light as much as possible, the incident light is off-central to the vial and the reflected light at $2\theta = 24^{o}$ is detected. The spectra were obtained as differential spectra between the spectra of samples stirred at 300 rpm and those of the same samples unstirred. Thus, the intensities of the different samples are incomparable with each other.

Gas sorption isotherm measurement. The adsorption isotherms of N_2 at 77 K and CO_2 at 273 K were carried out volumetrically on Belsorp. N_2 and CO_2 gases with high purity (99.99 %) were used. Prior to the adsorption isotherm measurements, the samples (around 30 mg) were outgassed under vacuum ($P < 10^{-4}$ Pa) for 2 h at 373 K.

AUTHOR INFORMATION

Corresponding Author

* Yoshiaki Uchida

E-mail: yuchida@cheng.es.osaka-u.ac.jp

ACKNOWLEDGMENT

This work was supported in part by the Japan Science and Technology Agency (JST) “Precursory Research for Embryonic Science and Technology (PRESTO)” for a project of “Molecular technology and creation of new function”. The TEM measurements were carried out by using a facility in the Research Center for Ultrahigh Voltage Electron Microscopy, Osaka University

Supporting Information Available: Figures S1 and S2.

REFERENCES

(1) Rogers, J. A.; Lagally, M. G.; Nuzzo, R. G. Synthesis, Assembly and Applications of Semiconductor Nanomembranes *Nature* **2011**, *477*, 45–53.

(2) MacEwan, D. M. C.; Wilson, M. J. In *Crystal Structures of Clay Minerals and Their X-ray Identification*; Brindley, G. W.; Brown, G., Eds.; Mineralogical Society of Great Britain and Ireland: Middlesex, United Kingdom, 1980; Chapter 3, p197.

(3) Ma, R.; Sasaki, T. Nanosheets of Oxides and Hydroxides: Ultimate 2D Charge–Bearing Functional Crystallites *Adv. Mater*. **2010**, *22*, 5082-5104.

(4) Liu, Y.; Wu, Z.; Zhang, H. Deriving the Colloidal Synthesis of Crystalline Nanosheets to Create Self–Assembly Monolayers of Nanoclusters *Adv. Colloid Interface Sci*. **2014**, *207*, 347-360.

(5) Rao, C. N. R.; Ramakrishna Matte, H. S. S.; Maitra, U. Graphene Analogues of Inorganic Layered Materials *Angew. Chem. Int. Ed*. **2013**, *52*, 13162-13185.

(6) Novoselov, K. S.; Geim, A. K.; Morozov, S. V.; Jiang, D.; Zhang, Y.; Dubonos, S. V.; Grigorieva, I. V.; Firsov, A. A. Electric Field Effect in Atomically Thin Carbon Films *Science* **2004**, *306*, 666–669.

(7) Chhowalla, M.; Shin, H. S.; Eda, G.; Li, L. J.; Loh, K. P.; Zhang, H. The Chemistry of Two–Dimensional Layered Transition Metal Dichalcogenide Nanosheets *Nat. Chem*. **2013**, *5*, 263–275.

(8) Nicolosi, V.; Chhowalla, M.; Kanatzidis, M. G.; Strano, M. S.; Coleman, J. N. Liquid Exfoliation of Layered Materials *Science* **2013**, *340*, 1226419.

(9) Qin, H. L.; Wang, D.; Huang, Z. L.; Wu, D. M.; Zeng, Z. C.; Ren, B.; Xu, K.; Jin, J. Thickness–Controlled Synthesis of Ultrathin Au Sheets and Surface Plasmonic Property *J. Am. Chem. Soc.* **2013**, *135*, 12544–12547.

(10) Malikova, N.; Pastoriza-Santos, I.; Schierhorn, M.; Kotov, N. A.; Liz-Marzan, L. M. Layer–by–Layer Assembled Mixed Spherical and Planar Gold Nanoparticles: Control of Interparticle Interactions *Langmuir* **2002**, *18*, 3694–3697.

(11) Zhou, M.; Chen, S.; Zhao, S.; Ma, H. Preparation of Gold Nanoplates by an Electrochemical Method *Chem. Lett.* **2005**, *34*, 1670–1671.

(12) Ibano, D.; Yokota, Y.; Tominaga, T. Preparation of Gold Nanoplates Protected by an Anionic Phospholipid *Chem. Lett.* **2003**, *32*, 574–575.

(13) Tsuji, M.; Hashimoto, M.; Nishizawa, Y.; Tsuji, T. Preparation of Gold Nanoplates by a Microwave–polyol Method *Chem. Lett.* **2003**, *32*, 1114–1115.

(14) Kim, J.-U.; Cha, S.-H.; Shin, K.; Jho, J.-Y.; Lee, J.-C. Preparation of Gold Nanowires and Nanosheets in Bulk Block Copolymer Phases under Mild Conditions *Adv. Mater.* **2004**, *16*, 459–464.

(15) Uchida, Y.; Nishizawa, T.; Omiya, T.; Hirota, Y.; Nishiyama, N. Nanosheet Formation in Hyperswollen Lyotropic Lamellar Phases *J. Am. Chem. Soc.* **2016**, *138*, 1103–1105.

(16) Horcajada, P.; Gref, R.; Baati, T.; Allan, P. K.; Maurin, G.; Couvreur, P.; Férey, G.; Morris, R. E.; Serre, C. Metal–Organic Frameworks in Biomedicine *Chem. Rev.* **2012**, *112*, 1232-1268.

(17) Chulkaivalsucharit, P.; Wu, X.; Ge, J. Synthesis of Enzyme–Embedded Metal–Organic Framework Nanocrystals in Reverse Micelles *RSC Adv.* **2015**, *5*, 101293–101296.

(18) Tsuruoka, T.; Furukawa, S.; Takashima, Y.; Yoshida, K.; Isoda, S.; Kitagawa, S. Nanoporous Nanorods Fabricated by Coordination Modulation and Oriented Attachment Growth *Angew. Chem. Int. Ed.* **2009**, *48*, 4739-4743.

(19) Sakata, Y.; Furukawa, S.; Kitagawa, S. Shape-Memory Nanopores Induced in Coordination Frameworks by Crystal Downsizing *Science* **2013**, *339*, 193-196.

(20) Sakamoto, R.; Takada, K.; Pal, T.; Maeda, H.; Kambecd, T.; Nishihara, H. Coordination nanosheets (CONASHs): strategies, structures and functions *Chem. Commun.* **2017**, *53*, 5781-5801.

(21) Michl, J.; Magnera, T. F. Two–Dimensional Supramolecular Chemistry with Molecular Tinkertoys *Proc. Natl. Acad. Sci. USA* **2002**, *99*, 4788-4792.

(22) Makiura, R.; Motoyama, S.; Umemura, Y.; Yamanaka, H.; Sakata, O.; Kitagawa, H. Surface Nano–Architecture of a Metal–Organic Framework *Nat. Mater.* **2010**, *9*, 565-571.

(23) Li, D.; Kaneko, K. Hydrogen Bond-Regulated Microporous Nature of Copper Complex–Assembled Microcrystals *Chem. Phys. Lett.* **2001**, *335*, 50–56.

(24) Kajiro, H.; Kondo, A.; Kaneko, K.; Kanoh, H. Flexible Two–Dimensional Square-Grid Coordination Polymers: Structures and Functions *Int. J. Mol. Sci.* **2010**, *11*, 3803-3845.

(25) Kondo, A.; Kajiro, H.; Noguchi, H.; Carlucci, L.; Proserpio, D. M.; Ciani, G.; Kato, K.; Takata, M.; Seki, H.; Sakamoto, M.; Hattori, Y.; Okino, F.; Maeda, K.; Ohba, T.; Kaneko, K.; Kanoh, H. Super Flexibility of a 2D Cu-Based Porous Coordination Framework on

Gas Adsorption in Comparison with a 3D Framework of Identical Composition: Framework Dimensionality–Dependent Gas Adsorptivities *J. Am. Chem. Soc.* **2011**, *133*, 10512–10522.

(26) Watanabe, S.; Ohsaki, S.; Hanafusa, T.; Takada, K.; Tanaka, H.; Mae, K.; Miyahara, M. T. Synthesis of Zeolitic Imidazolate Framework-8 Particles of Controlled Sizes, Shapes, and Gate Adsorption Characteristics Using a Central Collision–Type Microreactor *Chem. Eng. J.* **2017**, *313*, 724-733.

(27) Xu, M.; Yuan, S.; Chen, X.-Y.; Chang, Y.-J.; Day, G.; Gu, Z.-Y.; Zhou H.-C. Two-Dimensional Metal−Organic Framework Nanosheets as an Enzyme Inhibitor: Modulation of the α–Chymotrypsin Activity *J. Am. Chem. Soc.* **2007**, *139*, 8312-8319.

(28) Yamamoto, T.; Satoh, N.; Onda, T.; Tsujii, K. A Novel Iridescent Gel Phase of Surfactant and Order–Disorder Phase Separation Phenomena *Langmuir* **1996**, *12*, 3143-3150.

(29) Kobayashi, C.; Yamamoto, J.; Takanishi, Y. Photonic Effect in a Hyper–Swollen Lyotropic Lamellar Phase *J. Appl. Phys.* **2012**, *112*, 013531.

(30) Yang, J.; Yu, Q.; Zhao, Q.; Liang, J.; Dong, J.; Li, J. Adsorption CO_2, CH_4 and N_2 on Two Different Spacing Flexible Layer MOFs *Micropor. Mesopor. Mater*. **2012**, *161*, 154–159.

(31) Hiraide, S.; Tanaka, H.; Miyahara, M. T. Understanding Gate Adsorption Behaviour of CO_2 on Elastic Layer–Structured Metal–Organic Framework–11 *Dalton Trans.* **2016**, *45*, 4193–4202.

TOC graphic

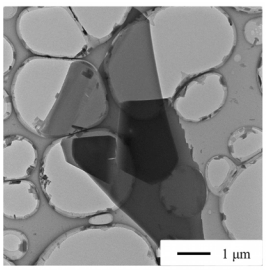
1 μm

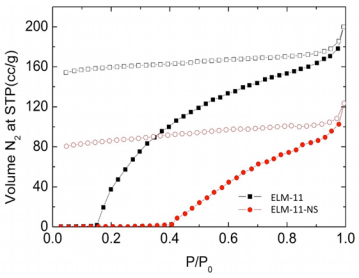
Volume N2 at STP(cc/g)
P/P0
ELM-11
ELM-11-NS
0
40
80
120
160
200
0.0
0.2
0.4
0.6
0.8
1.0